Chinese Journal of
POLYMER SCIENCE

ARTICLE

https://doi.org/10.1007/s10118-018-2100-4
Chinese J. Polym. Sci.

Structures and Surface States of Polymer Brushes in Good Solvents: Effects of Surface Interactions

Yi-Xin Liu* and Hong-Dong Zhang

State Key Laboratory of Molecular Engineering of Polymers, Department of Macromolecular Science, Fudan University, Shanghai 200433, China

Abstract The influence of the surface interaction on the mesoscopic structure of grafted polymers in good solvents has been examined. At high surface coverage, tethered polymers are in the brush state and the parabolic segment density profile is confirmed by self-consistent field theory (SCFT) calculations. It is found that this is a universal behavior for a whole range of surface interactions from complete repulsion to strong attraction. More interestingly, finite surface repulsion may lead to the maximum in the proximal layer of its segment density profile, which is significantly different from both the depletion layer of pure repulsion and the adsorbing layer of attraction. In addition to the brush state on both repulsive and attractive surfaces, three additional surface states were identified by analyzing the scaling behavior of the layer thickness of polymer brushes: the mushroom state on repulsive substrates, the dilute and the semidilute surface states on attractive substrates.

Keywords Self-consistent field theory; Scaling theory; Polymer thin film; Polymer brush

Citation: Liu, Y. X.; Zhang, H. D. Structures and Surface States of Polymer Brushes in Good Solvents: Effects of Surface Interactions. Chinese J. Polym. Sci. https://doi.org/10.1007/s10118-018-2100-4

INTRODUCTION

Polymer brushes, being polymer chains with one end tethered to solid surfaces or interfaces by covalent bonds, have attracted constant attention due to its fundamental importance in vast applications including templating for directed self-assembly (DSA), colloidal stablization, smart materials as well as bio-related applications such as anti-biofouling and biosensing[1–9]. After the pioneering work of Alexander[10] and de Gennes[11], many theoretical methods in addition to the scaling analysis have been introduced to investigate both static and dynamic properties of polymer brushes. Some prominent examples are the strong stretching theory (SST) of Milner[12, 13], the classical theory accounting for finite stretching derived by Netz and Schick[14], and self-consistent field theory (SCFT)[15, 16]. Owing to these efforts together with computer simulations and experiments, the theory of polymer brushes at least on impenetrable and purely repulsive flat surfaces is well developed[2]. In practice, however, purely repulsive surfaces, as often assumed in analytical theories, are hard to prepare. In many situations, such as wetting, adsorption and capillarity, the interfacial energy, which characterizes the interaction between surfaces and polymer monomers, cannot simply be ignored. In fact, studies of polymers adsorbed but not tethered to attractive surfaces give some hints: the surface interaction can significantly perturb the near-surface structure of polymers[17]. In contrast to absorbed polymers, tethered polymers are able to stay even on the repulsive surfaces due to their covalent bonds with the surface and the surface density can be increased well beyond the value achievable by adsorption effects alone.

Despite the significance of the presence of surface interaction, much less attention has been focused on its influence on the structure of polymer brushes, especially for the case of weakly repulsive interactions. The scaling theory for isolated tethered polymers on attractive surfaces has been developed by Eisenriegler and coworkers[18]. They found that a surface phase transition occurs even for a single chain system. Later, this treatment was extended to the case of repulsive surfaces[19] and to many-chain systems with a full range of surface density from dilute to over saturation[20, 21]. The scaling forms of segment density profile (along the grafting surface normal) and the layer thickness of polymer brushes were obtained using scaling analysis. Under good solvent condition, up to six surface states of tethered polymers on interacting surfaces (both repulsive and attractive) were predicted by Descas, Sommer and Blumen[21]. They are the brush and the mushroom states on the repulsive surface and the dilute, the semidilute, the oversaturated adsorbed and the oversaturated brush states on the attractive surface. These results have also been verified by Monte Carlo simulations[21].

Several attempts based on field theoretic approaches have been made to treat the problem of polymer brushes considering the surface interaction effects. Douglas and

* Corresponding author: E-mail lyx@fudan.edu.cn

Received November 23, 2017; Accepted December 3, 2017; Published online February 28, 2018

coworkers[22] adopted renormalization group (RG) theory to calculate the segment density in the dilute surface regime, while analytical SCFT in the strong stretching limit was used by Marko and colleagues[23] to discuss the structure of polymer brushes in the brush state. Numerical SCFT methods have also been considered but only lattice formulation was implemented to study polymer brushes on the attractive surface[24]. To model the surface interaction in field theoretic simulations, such as in SCFT, a common approach is to introduce an arbitrary surface potential which should be convenient for numerical computations. Nevertheless, this approach may require high spatial resolution near the surface to model the repulsive part of the surface potential, which would make the computation too expensive. A preferable alternative approach is to use an effective boundary condition which avoids resolving the surface potential explicitly[25]. However, such boundary conditions are usually non-periodic, which renders Fourier based pseudo-spectral methods, such as that in Ref. [26], inapplicable in solving the modified diffusion equations (MDEs). Recently, we have developed a highly efficient algorithm, ETDRK4[27], which can handle general non-periodic boundary conditions, such as the Robin boundary condition (RBC), and still retain the spectral accuracy as in the conventional pseudo-spectral algorithms[28, 29].

So far, we are not aware of any report on numerical SCFT in the continuum limit that treats the surface interaction between polymer brushes and grafting surfaces in a consistent manner. Despite this, SCFT provides much more details about the segment profile and the end-segment distribution. And in principle, it can be generalized to different solvent conditions and mixed brushes as well as polymer chains with various chain architectures, as compared with scaling theories. In this paper, we utilize our recently developed tool to solve the SCFT problem of homopolymer brushes in good solvents on interacting surfaces. The effects of surface interactions, the excluded volume interaction and the grafting density on the structure of polymer brushes are carefully examined. Five distinct surface states of polymer brushes on the interacting surfaces have been identified by analyzing the scaling relation between the layer thickness and the stretching parameter (β) as a function of the surface interaction.

NUMERICAL METHODS

We consider n polymer chains, each comprising N identical statistical segments of length b, are randomly and permanently tethered to a flat, impenetrable surface (wall). The tethered polymers are immersed in good solvents and the total volume of the system is $V = L_z L_\perp^2$, where L_z and $L_\perp$ are the length of the system along z direction which is normal to the grafting surface and lateral size, respectively. The grafting density is defined as number of polymer segments per unit area, $\sigma = nN/L_\perp^2$. We adopt the SCFT description of such kind of system and the set of SCFT equations and their derivation details can be found in Refs. [25] and [30]. In particular, polymers are modeled as continuous Gaussian chains and solvent molecules are implicitly treated as an excluded volume interaction with polymer segments. Note that such implicit treatment of solvents has some limitations because only binary interactions are considered. This model is valid only when the polymer concentration is low enough. It is recommended to refer to, for example, Ref. [31] for a detailed discussion.

We numerically solve the set of SCFT equations using a self-consistent scheme in which the solution of modified diffusion equations (MDEs) is the most time-consuming step. To efficiently handle non-periodic boundary conditions in the MDEs, we discretize spatial variables on a one dimensional Chebyshev-Gauss-Lobatto (CGL) grid with a set of grid points $z_j = \cos\left(\frac{\pi j}{N_z}\right), j = 0, 1, \ldots, N_z$. Then the MDEs are solved by a fourth order time stepping method, ETDRK4, which performs extremely well for SCFT calculations as shown in our previous study[27]. The numerical details, tweaks, and performance of this method can be found elsewhere[27].

The initial boundary condition arising from the grafting points of the polymer brushes contains a Dirac delta function, which brings additional difficulty that it will deteriorate the convergence properties and produce oscillations in the self-consistent fields and density profiles[26, 32]. Several numerical approximations for the Dirac delta functions have been considered and their performance were examined carefully, including the Kronecker delta[32], a Gaussian distribution with very narrow peak width[26], the derivative of the Heaviside function, and an approach that propagates one contour step using an integral form corresponding to the MDE[32]. After comparison of these approaches, we choose the last one that is the most accurate and shows excellent stability.

The normalized single chain partition function Q and the mean-field free energy F, both of which can be expressed as spatial integrals, are evaluated by the Clenshaw-Curtis quadrature scheme[33], which converges exponentially on the CGL grid. Finally, a continuously steepest descent algorithm is used to relax potential fields to the equilibrium state, *i.e.* the saddle point of the set of SCFT equations[25].

RESULTS AND DISCUSSION

Polymer-surface Interactions

Among all energy contributions, we will pay particular attention to the polymer-surface interactions. We assume that polymer-surface interactions are short-ranged and only binary interactions are important. Generally, given the potential energy per segment $\varphi(z)$ which is normalized according to $\int \mathrm{d}z\varphi(z) = 1$, the Hamiltonian for polymer-surface interactions can be written as[23]

$$H_s = \int \mathrm{d}^3\mathbf{r}\Gamma_s\varphi(z)\rho(\mathbf{r}) \quad (1)$$

where Γ_s is a parameter that measures the total surface interactions and $\rho(\mathbf{r})$ denotes the segment density at position $\mathbf{r}$. To gain a qualitative knowledge about Γ_s, it is helpful to introduce a $\varphi(z)$ being a simplified form for the van der Waals interaction, *i.e.* $\varphi(z) = +\infty$ when $z > \sigma_s$, otherwise

$\varphi(z) = -\varphi_0(\sigma_s/z)^6$. By analogy to the theory of real gas, we can obtain the magnitude of the integral binary surface potential

$$\Gamma_s = \sigma_s\left(1 - \frac{\varphi_0}{k_B T}\right) \quad (2)$$

The above relation is in essential the same as that derived by Douglas *et al.*[34] if we replace φ_0/k_B by θ_A. Obviously, θ_A is a temperature that makes Γ_s vanish. In other words, it denotes a compensation point where attractions between the surface and polymer segments exactly cancel out entropic repulsions experienced by polymer segments near an impenetrable wall[22]. By lowering the temperature, or alternatively raising θ_A (making the potential well deeper), Γ_s tends to be negative indicating that the grafting surface attracts polymers. Oppositely, positive Γ_s corresponds to the case of a repulsive surface. In the limit of $\Gamma_s \to \infty$, polymer segments are completely repelled by the grafting surface.

In this study, we consider a surface potential of the form $\varphi(z) = \delta(z)$, which is a delta function situated at $z = 0$. It has been demonstrated that the delta function surface potential can model any particular $\varphi(z)$ by appropriately chosen Γ_s at least in the situation under the ground state dominance approximation[35]. Therefore we can conveniently consider the delta function surface potential as an effective surface potential for all binary surface interactions. According to de Gennes[17] and Wu *et al.*[35], the statics of a polymer in the delta function surface potential can be described by a Robin boundary condition on the diffusion equation at the grafting surface of the following form

$$\frac{\partial q}{\partial s}|_{z=0} = -\kappa_a q|_{z=0} \quad (3)$$

where $q = q(\mathbf{r}, s)$ is a propagator function which represents the spatial probability distribution of the segment of length s along the chain contour from the starting segment ($0 \le s \le N$). In Eq. (3), $\kappa_a = -3\Gamma_s/a^2$ and clearly its absolute reciprocal value κ_a^{-1} is a length scale that characterizes the net strength of the surface interactions. Note that κ_a has an opposite sign of Γ_s, meaning that negative κ_a corresponds to the case of repulsive grafting surfaces and vice versa. As for the polymer/air interface, the boundary condition can be similarly imposed by replacing κ_a and $z = 0$ in Eq. (3) with κ_b and $z = L_z$, respectively, where κ_b^{-1} is another length scale that characterizes the strength of the surface interactions at polymer/air interface. In this study, we will not consider the polymer/air interactions and $\kappa_b = -\infty$ is assumed throughout. Furthermore, the box size L_z is chosen large enough to avoid any unnecessary effects caused by the polymer/air interface.

To circumvent the difficulty of Robin boundary conditions and other non-periodic boundary conditions encountered in the numerical solution of SCFT equations, we introduce the Chebyshev-Gauss-Lobatto (CGL) grid other than uniform grid, and collocate all spatial variables on the grid. The modified diffusion equations are then solved by an exponential time differencing method combined with a fourth order Runge-Kutta scheme (ETDRK4) based on the Chebyshev series expansion. In our previous study[27], we have demonstrated that this numerical approach is superior to equispaced grid based methods due to its high resolution near boundaries. And it is also more efficient than the operator splitting method coupled with Chebyshev series expansion developed by Hur *et al.*[36] owing to its better convergent properties and less time demanding operations.

Structures of Polymer Brushes

By considering the grafting surface as an impenetrable wall and ignoring any surface interactions, the Alexander box model of polymer brushes predicts that the brush thickness scales as $N\sigma^{1/3}$[10, 11]. Thus it is natural to rescale all length quantities with respect to $\hat{z} = N\sigma^{1/3}\left(2v_0a^2/3\right)^{1/3}$ to make them dimensionless, where v_0 is the exclude volume of a polymer segment which characterizes the strength of interactions between polymer segments and solvent molecules. With dimensionless exclude volume $\bar{v}_0 = v_0N^2/R_g^3$ and grafting density $\bar{\sigma} = \sigma R_g^2/C$ it can be expressed more compactly as $\hat{z} = (4\bar{v}_0\bar{\sigma}C)^{1/3}R_g$, where $C = \rho_0 R_g^3/N$ is an important parameter that signifies the validity of mean-field approximation (ρ_0 is the average segment number density). Meanwhile, we introduce a dimensionless, rescaled, segment density $\phi = \rho/\hat{\rho}$ with $\hat{\rho} = N\sigma/\hat{z}$ being the averaging segment density over $\hat{z}$.

For homopolymers tethered to a neutral impenetrable surface where $\kappa_a \to -\infty$, it has been shown by Netz and Schick[14] that the only parameter remaining in SCFT is the stretching parameter $\beta \equiv (\bar{w}\bar{\sigma}C/2)^{2/3} = \left(\hat{z}/2R_g\right)^2$, which measures the degree of polymer chains being stretched. For $\beta \ll 1$, tethered polymers are in the so-called "mushroom" state. The height of the polymers tends to be the size of the unperturbed polymer coil, thus significantly larger than the typical length scale $\hat{z}$. When β is large enough, tethered chains feel the exclude volume interactions from neighboring chains, leading to the "brush" state. Therefore, there is a mushroom to brush transition along increase of β. In the limit of infinite stretching, $\beta \to \infty$, density profiles from SCFT calculations approach the prediction of strong stretching theory (SST), as demonstrated in Fig. 1 and in the work of Netz and Schick[14]. SST also predicts a constant dimensionless brush height of $\frac{3}{8}\left(\frac{6}{\pi^2}\right)^{1/3} \approx 0.32$, which means that the brush height is on the order of $\hat{z}$, while our SCFT calculations given in the inset of Fig. 1 show that the dimensionless brush height depends on β and gradually approaches to the predicted value. The dimensionless brush height $h/\hat{z}$ decreases with the increase of β, which seems to counter the fact that the brush height h should increase as the grafting density σ increases. We should point out that the opposite behavior is caused by the fact that both $\hat{z}$ and β are dependent on σ. This result is consistent with that revealed by the off-lattice Monte Carlo simulation[37]. Note that exact value of the layer thickness of tethered polymers depends on its definition. In this study, the layer thickness is defined as

$$h = \frac{\int dz\, z\phi(z)}{\int dz\, \phi(z)} \quad (4)$$

while in the SST it is common to choose the height where the polymer density approaches zero, denoted as

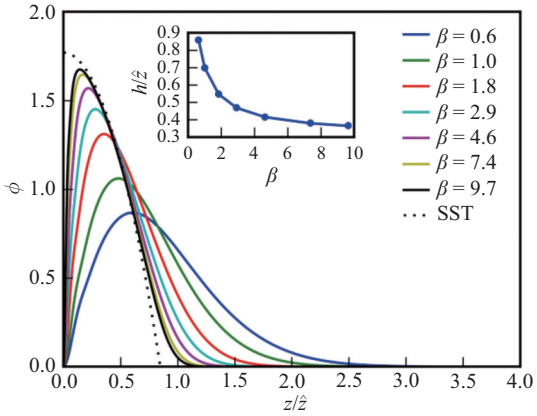

Fig. 1 Rescaled density profiles as a function of the rescaled distance from the grafting surface along the surface normal calculated by SCFT with Dirichlet boundary condition ($\kappa_a \to -\infty$) at grafting surfaces. The dash line profile, $\phi(z) = (3\pi/4)^{2/3} - (\pi z/2)^2$, is the result of SST. The inset plots the layer thickness as a function of β, where the horizontal solid line is the prediction of SST.

$z_m = \left(\frac{6}{\pi^2}\right)^{1/3}$ [14]. Consequently, the layer thickness at SST using definition as in Eq. (4) is only $\frac{3}{8}$ of z_m. Like the numerical results of Netz and Schick[14], we also observe a depletion layer near the grafting surface and an exponentially decaying tail far away from the grafting surface. The numerical results confirm that length scales of these two regions over the brush height become vanishingly small as $\beta \to \infty$. Note that SST corresponds to the case of SCFT when the wall is purely repulsive (*i.e.* $\kappa_a \to -\infty$) and $\beta \to \infty$.

For homopolymers tethered to an interacting surface where κ_a is finite, grafted polymers will eventually evolve into the brush state as β increases no matter whether the grafting surface is repulsive or attractive. Segment density profiles obtained from our SCFT calculations for four typical surface affinities are presented in Fig. 2, where the parabolic feature in profiles at large β clearly indicates the emergence of the brush state. For attractive surface, as shown in Fig. 2(d), at low β density profiles resemble those of adsorbed polymers[19]. In this regime, polymer chains are fully adsorbed on the surface. Each chain consists of a string of adsorption blobs containing g segments each. These blobs form a quasi-two dimensional layer on the surface. This layer thickness defines another characteristic length $D = g^{\nu}a$ which scales as $\kappa_a^{-\nu/\varphi}$ in addition to the size of polymers in the good solvent $R_F = N^{\nu}a$, where ν is the Flory exponent for real chains in good solvents and φ is the surface crossover exponent[21]. In our SCFT calculations, the adsorption length D actually decreases by enhancing the surface attraction κ_a. A log-log plot of the density profiles in Fig. 2(d) shows that the density obeys a power law $\phi(z) \sim z^{-1/3}$ for $a < z < D$, indicating a self-similar structure of tethered polymers near the grafting surface. This observation agrees well with the prediction of the scaling theory[19, 38]. It is interesting to mention that the proximal behavior of the segment density

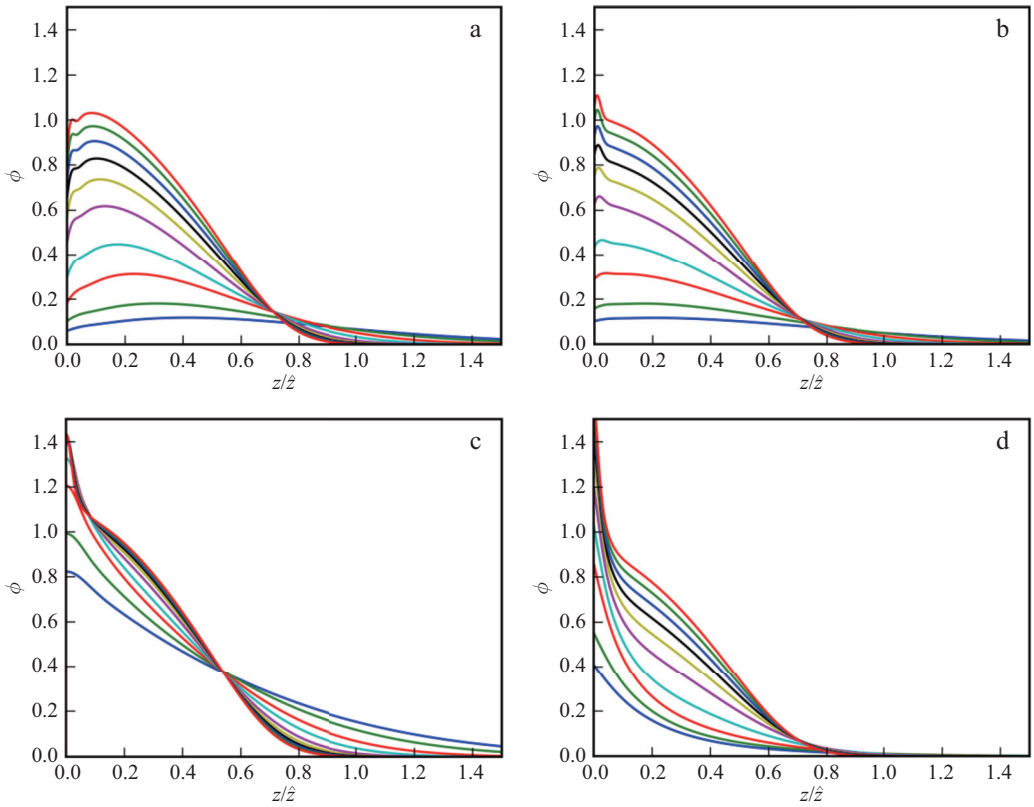

Fig. 2 Rescaled segment density profiles as a function of the rescaled distance from the grafting surface calculated by SCFT with (a) $\kappa_a = -10$, (b) $\kappa_a = -4$, (c) $\kappa_a = 0$, and (d) $\kappa_a = 5$. For each part, the values of β for profiles from bottom to top are 0.6, 1.0, 1.8, 2.9, 4.6, 6.1, 7.4, 8.5, 9.7, and 10.7, respectively.

https://doi.org/10.1007/s10118-018-2100-4

does not change with β. This should be clearly seen in Fig. 2(d) for β greater than 2.9 when the parabolic feature begins to develop—for each β profile the parabolic feature starts at nearly the same distance from the grafting surface. It is understandable that the adsorption blob is solely controlled by the surface interaction but not by the effective surface coverage. To see that there is actually a transition from the adsorbed state to the brush state, we plot the distribution function of free end segments in Fig. 3(b). The distribution function should decrease monotonously in the adsorbed state while it will have a smooth maximum in the brush state. As can be seen in Fig. 3(b) for $\kappa_a = 5$, the maximum emerges at $\beta = 3.8$ and becomes more and more pronounced as β increases.

For repulsive wall, we have observed depletion layers for all $\kappa_a < 0$ we studied. It is believed that the conformation of tethered polymers is dominated by entropic effects and it is basically isotropic[20, 21]. This suggests that the segment density should be similar to that of the purely repulsive case—there is only one broad and smooth maximum located at distance R_F in mushroom state and the maximum moves toward the surface in the brush state as β increases. However, in our SCFT results shown in Figs. 2(a) and 2(b), two maxima can be identified, where the one near the wall is captured neither by the previous scaling analysis[19] nor by mean-field studies[39] and renormalization group methods[22], but we do notice some evidences of the first maximum in the results of Monte Carlo simulations reported by Grest[40]. At the same κ_a the position of the first maximum z_r does not change with β, while it shifts to the wall as κ_a increases.

More interestingly, the shift trend of the first maximum seems to continue as κ_a turns from negative to positive. The first maximum exactly locates at the wall when $\kappa_a = 0$ (see Fig. 2), indicating $z_r = 0$. As κ_a keeps on going to positive, the maximum can be viewed as being shifted to the other side of the wall with $z_r < 0$, thus the maximum is no longer visible at the range $z > 0$. We infer from this observation that the first maximum is produced mainly by the polymer-surface interactions, for there is always a proximal layer near the wall for any κ_a. The difference of the density profile in the proximal layer is due to different conformations that the polymer chain takes. The fact that the density is maximized inside the proximal layer for the repulsive wall implies that polymers take blob-like conformations whose center corresponds to the position of the density maximum. The density maximum disappears for the attractive wall because polymers in the proximal layer also take blob-like conformations but their center locate somewhere inside the wall. In this case, the conformation looks like a spherical cap lying on the grafting surface. Note that Flatt *et al.*[41] also proposed a similar model for comb copolymers adsorbed on attractive surfaces. Using scaling analysis, de Gennes and Eisenriegler found that the density profile of the depletion layer for purely repulsive case ($\kappa_a \to -\infty$) may be described by the scaling form $\phi(z) \sim z^{1/\nu}$ and it obeys the scaling form $\phi(z) \sim z^{-1/3}$ for attractive case ($\kappa_a > 0$), respectively. For finite negative κ_a, here we assume that the former scaling form controls the region $0 < z < z_r$ and the later scaling form dominates the region $z > z_r$ until the border of the proximal layer is touched. Therefore, the density maximum in the proximal layer is a direct consequence of the combination of these two scaling laws.

For finite negative κ_a the repulsion of the wall is not strong enough that the segment density at the wall $\phi_s = \phi(z = 0)$ does not vanish. ϕ_s increases as κ_a becomes less negative, *i.e.* weakening of the repulsion of the wall, as expected. In Fig. 3(a), it is easy to notice that there are a certain amount of end segments on the wall even when the wall is repulsive. However, the end-segment distribution contains only one smooth maximum for both low and high β unlike the segment density profile that generally has two maxima.

Surface States of Polymer Brushes

Further analysis of the density profile by measuring the thickness of the tethered polymers leads to the identification of various regimes of surface states in β-κ_a parameter space. The main results are presented in Fig. 4 where $\lg(h/R_g)$ is plotted as a function of $\lg\beta$ for different surface affinities including both negative and positive κ_a. As mentioned in the above section, for repulsive wall while $\kappa_a < 0$, there is a mushroom-brush transition. For low β in the mushroom state, the layer thickness is essentially the size of polymer coil in good solvents which should not vary with β. This is confirmed in the top left corner of Fig. 4 for $\kappa_a = -\infty, -40,$

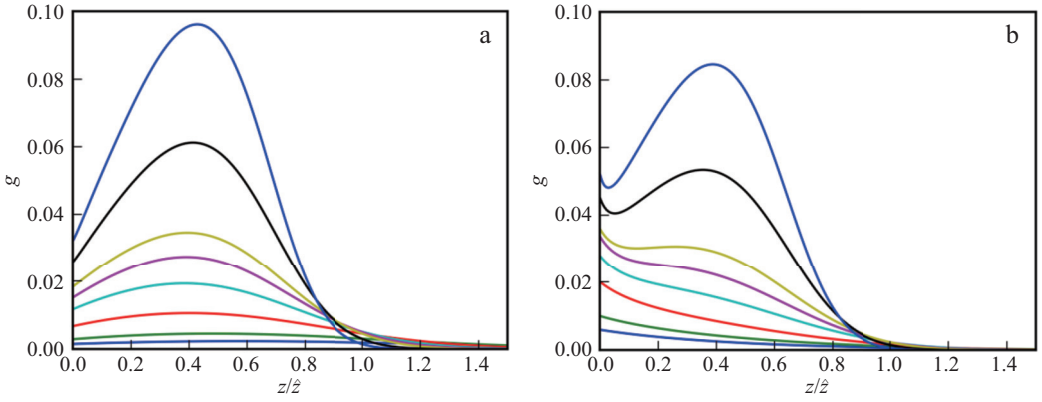

Fig. 3 Distribution function of end segments calculated by SCFT with (a) $\kappa_a = -4$ and (b) $\kappa_a = 5$. Profiles in both (a) and (b) from bottom to top correspond to $\beta = 0.6$, 1.0, 1.8, 2.9, 3.8, 4.6, 7.4, and 10.7, respectively.

https://doi.org/10.1007/s10118-018-2100-4

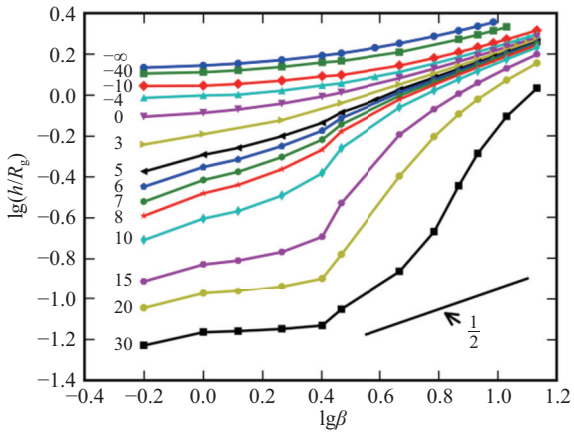

Fig. 4 The logarithm of brush heights in unit of R_g as a function of the logarithm of the parameter β for different surface affinities of the grafting surface. The numbers listed in the left of profiles are the values of κ_a. The straight line at the right bottom corner indicates the power law $h/R_g \sim \beta^{1/2}$.

−10, and −4. When β is large enough to enter the brush state, it is well established that the brush thickness should obey the scaling law $h/R_g \sim N(v_0\sigma)^{1/3}$. And using the definition of β we have $h/R_g \sim \beta^{1/2}$. This scaling law is well approached as can be seen in the top right corner of Fig. 4.

For $\kappa_a > 0$, one can identify three distinct regions in Fig. 4. When β is large enough, tethered polymers are in the brush state thus the layer thickness obeys the same scaling law $h/R_g \sim \beta^{1/2}$ as that of repulsive case. As can be seen in Fig. 2(d), the adsorbed layer consumes a significant amount of segments which are expected to form brush. Therefore, the brush thickness should be smaller than the brush formed on the repulsive wall and it is supposed to depend on both β and κ_a in the following form[23],

$$h = h_0\left(1 - \frac{\kappa_a}{N\sigma}\right)^{\frac{1}{3}} \tag{5}$$

where h_0 is the brush thickness in the absence of attractive surface interactions. If we rewrite Eq. (5) in the form $(h/\hat{z})^3 = c\left(1 - b\kappa_a\beta^{-3/2}\right)$ where the relation $h_0 \sim \hat{z}$ is used and c, b are some constants, we expect a linear relation between $(h/\hat{z})^3$ and $\beta^{-3/2}$. By plotting $(h/\hat{z})^3$ as a function of $\beta^{-3/2}$ shown in Fig. 5(b), we actually observe the linear dependence at the large β region for all $\kappa_a > 0$ we studied. Moreover, the slope of the straight part becomes deeper as κ_a increases in consistent with Eq. (5).

When κ_a and β are both small, as in the middle left part of Fig. 4, the layer thickness seems to also obey the scaling law $h/R_g \sim \beta^{1/2}$ or equivalently $h \sim \hat{z}$. The scaling law is further confirmed by plotting the scaled layer thickness $h/\hat{z}$ as a function of κ_a for several small β (see Fig. 5a). Almost all data points for different β in the range of $5 < \kappa_a < 15$ collapse onto a universal curve. The scaling law, however, has a very different origin than that of the brush state. A possible interpretation based on scaling analysis of this scaling law is given below. We assume in this regime tethered polymers are in the semidilute surface state where the grafting density exceeds a critical grafting density σ^* at which the adsorbed chains start to overlap. According to Bouchaud and Daoud[20], σ^* can be written as $\sigma^* \sim N^{-2\nu_2}\kappa_a^{-(\nu_2-\nu)/\varphi}$ where $\nu_2 = 3/4$ is the 2D Flory exponent. The layer thickness has the scaling structure $h/h_0 = f(\sigma/\sigma^*)$ with h_0 being the layer thickness when $\sigma \ll \sigma^*$[21]. At one limit $\sigma/\sigma^* \to 0$, the function f approaches 1 thus $h = h_0$. Meanwhile, at such low surface coverage, chains are all adsorbed on the wall and we have $h_0 = D$. At the other limit $\sigma \gg \sigma^*$ but not yet large enough to form brush, the loops and tails form an extended layer in addition to the proximal layer, whose characteristic size is that of an unperturbed chain, that is, $h = R_g \sim N^{1/2}$. Combining these two limits, we have the relation $N^{1/2} \sim Df(\sigma/\sigma^*)$ which can be satisfied only when f obeys a power law by noticing that D is independent of N. Equating the exponents of N from both side, we obtain the scaling law $h \sim \sigma^{1/4\nu_2} = \sigma^{1/3}$. Since σ is related to β as $\beta \sim \sigma^{2/3}$, the relation between layer thickness and β is finally achieved.

In the third regime of polymers grafted on the attractive wall, κ_a is large and β is low. The change of the layer

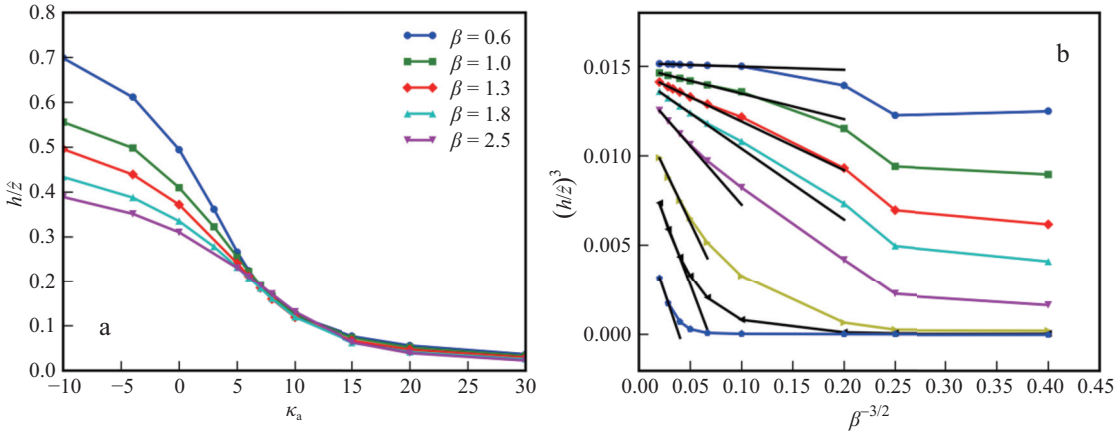

Fig. 5 The scaling regimes of brush heights of polymers tethered to absorbing surfaces: (a) The rescaled brush heights as a function of κ_a for some small βs which are listed in the legend; (b) The rescaled brush heights as a function of β for different κ_a (The curves from top to bottom correspond to κ_a = 5, 6, 7, 8, 10, 15, 20, and 30, respectively. The solid straight lines are linear fittings for first few data points for each κ_a.)

https://doi.org/10.1007/s10118-018-2100-4

thickness with β for different κ_a is shown in the lower left corner of Fig. 4. We can see that the layer thickness is almost constant with increasing β, indicating that tethered polymers are strongly attracted to the wall and they are in the dilute surface state. In this regime, the layer thickness is D, the size of adsorption blobs which does not depend on β as already discussed in the section before.

Apart from the above three states for the case of $\kappa_a > 0$, we also noticed that there was a crossover region where β was intermediate. Moreover, this region expands as κ_a increases. Descas, Sommer and Blumen[21] also predict a similar state, which they named the oversaturated adsorbed state, that it exists in a narrow region between the semidilute surface state and the oversaturated brush state.

CONCLUSIONS

In summary, we have demonstrated that surface interactions significantly impact the structure of tethered polymers by using SCFT calculations. In the limit of complete repulsion, there is a depletion layer of polymer segments near the wall. As the surface interaction goes from repulsive to attractive, the segment density at the wall increases monotonously. For attractive wall, the segment density decreases monotonously away from the wall. For weakly repulsive wall, two maxima are present in the segment density profile, among which the one closer to the wall corresponds to the center of the proximal layer and the other corresponds to the center of the polymer coil or the position the brush starts to develop. The scaling law of the density profile near the wall agrees well with the scaling analysis. By analyzing the scaling law of the layer thickness, up to five surface states of polymer brushes are identified in the parameter space of β and κ_a. For both repulsive and attractive wall, the brush state can be achieved either by enhancing the excluded volume interactions or by increasing the grafting density, *i.e.* by increasing β. In the brush state, the layer thickness scales as $\beta^{1/2}$. For repulsive wall and low β, polymers are in the mushroom state whose layer thickness does not change with β. For attractive wall and low β, two states are possible according to the strength of the surface interaction. For strong attractions, polymers are in the dilute state whose layer thickness is determined by the adsorption blob size which is independent of β. For relatively weak attractions, the layer thickness also obeys a one half power law of β but with a very different origin and polymers are in the semidilute surface state. A straightforward extension of this work is to carry out studies of the lateral structures of mixed brushes and block copolymer brushes on interacting surfaces and polymers tethered to curved interacting surfaces.

ACKNOWLEDGMENTS

This work was financially supported by the National Natural Science Foundation of China (No. 21004013).

REFERENCES

1 Chen, W. L.; Cordero, R.; Tran, H.; Ober, C. K. 50th Anniversary perspective: polymer brushes: novel surfaces for future materials. Macromolecules 2017, 50(11), 4089−4113.
2 Binder, K.; Milchev, A. Polymer brushes on flat and curved surfaces: how computer simulations can help to test theories and to interpret experiments. J. Polym. Sci., Part B: Polym. Phys. 2012, 50(22), 1515−1555.
3 Azzaroni, O. Polymer brushes here, there, and everywhere: Recent advances in their practical applications and emerging opportunities in multiple research fields. J. Polym. Sci., Part A: Polym. Chem. 2012, 50(16), 3225−3258.
4 Cohen Stuart, M. A.; Huck, W. T. S.; Genzer, J.; Müller, M.; Ober, C.; Stamm, M.; Sukhorukov, G. B.; Szleifer, I.; Tsukruk, V. V.; Urban, M.; Winnik, F.; Zauscher, S.; Luzinov, I.; Minko, S. Emerging applications of stimuli-responsive polymer materials. Nat. Mater. 2010, 9(2), 101−113.
5 Ayres, N. Polymer brushes: applications in biomaterials and nanotechnology. Polym. Chem. 2010, 1(6), 769−777.
6 Brittain, W. J.; Minko, S. A structural definition of polymer brushes. J. Polym. Sci., Part A: Polym. Chem. 2007, 45(16), 3505−3512.
7 Currie, E. P. K.; Norde, W.; Cohen Stuart, M. A. Tethered polymer chains: surface chemistry and their impact on colloidal and surface properties. Adv. Colloid Interface Sci. 2003, 100-102, 205–265.
8 Granick, S. Macromolecules at surfaces? research challenges and opportunities from tribology to biology J. Polym. Sci., Part B: Polym. Phys. 2003, 41(22), 2755−2793.
9 Halperin, A.; Tirrell, M.; Lodge, T. Tethered chains in polymer microstructures. Adv. Polym. Sci. 1992, 100, 31−71.
10 Alexander, S. Adsorption of chain molecules with a polar head a scaling description. J. Phys. 1977, 38(8), 983−987.
11 de Gennes, P. G. Conformations of polymers attached to an interface. Macromolecules 1980, 1075(19), 1069−1075.
12 Milner, S. T.; Witten, T.; Cates, M. Theory of the grafted polymer brush. Macromolecules 1988, 21(10), 2610−2619.
13 Milner, S. T. Polymer brushes. Science 1991, 251, 905−914.
14 Netz, R. R.; Schick, M. Polymer brushes: from self-consistent field theory to classical theory. Macromolecules 1998, 31(15), 5105−5122.
15 Wijmans, C. M.; Scheutjens, J. M. H. M.; Zhulina, E. B. Self-consistent field theories for polymer brushes: lattice calculations and an asymptotic analytical description. Macromolecules 1992, 25(10), 2657−2665.
16 Matsen, M. W.; Griffiths, G. H. Melt brushes of diblock copolymer. Eur. Phys. J. E 2009, 29(2), 219−227.
17 de Gennes, P. G., "Scaling concepts in polymer physics", Cornell University Press, Ithaca, 1979.
18 Eisenriegler, E.; Kremer, K.; Binder, K. Adsorption of polymer chains at surfaces: scaling and Monte Carlo analyses. J. Chem. Phys. 1982, 77(12), 6296−6320.
19 Eisenriegler, E. Dilute and semidilute polymer solutions near an adsorbing wall. J. Chem. Phys. 1983, 79(2), 1052−1064.
20 Bouchaud, E.; Daoud, M. Polymer adsorption: concentration effects. J. Phys. 1987, 48(11), 1991−2000.
21 Descas, R.; Sommer, J. U.; Blumen, A. Grafted polymer chains interacting with substrates: computer simulations and scaling. macromol. Theory Simul. 2008, 17(9), 429−453.
22 Adamuti-Trache, M.; McMullen, W. E.; Douglas, J. F. Segmental concentration profiles of end-tethered polymers with excluded-volume and surface interactions. J. Chem. Phys. 1996, 105(11), 4798−4811.
23 Marko, J. F.; Johner, A.; Marques, C. M. Grafted polymers under the influence of external fields. J. Chem. Phys. 1993, 99(10), 8142−8153.
24 Bijsterbosch, H. D.; de Haan, V. O.; de Graaf, A. W.; Mellema, M.; Leermakers, F. A. M.; Cohen Stuart, M. A.; van Well, A. A. Tethered adsorbing chains: neutron reflectivity and surface pressure of spread diblock copolymer monolayers. Langmuir

1995, 29(14), 4467−4473.
25 Fredrickson, G.H., "The equilibrium theory of inhomogeneous polymers", Clarendon Press, Oxford, 2006.
26 Chantawansri, T. L.; Hur, S. M.; García-Cervera, C. J.; Ceniceros, H. D.; Fredrickson, G. H. Spectral collocation methods for polymer brushes. J. Chem. Phys. 2011, 134(24), 244905.
27 Liu, Y. X.; Zhang, H. D. Exponential time differencing methods with Chebyshev collocation for polymers confined by interacting surfaces. J. Chem. Phys. 2014, 140(22), 224101.
28 Rasmussen, K. Ø.; Kalosakas, G. Improved numerical algorithm for exploring block copolymer mesophases.. J. Polym. Sci., Part B: Polym. Phys. 2002, 40(16), 1777−1783.
29 Tzeremes, G.; Rasmussen, K. Ø.; Lookman, T.; Saxena, A. Efficient computation of the structural phase behavior of block copolymers. Phys. Rev. E. 2002, 65(4), 041806.
30 Müller, M. Phase diagram of a mixed polymer brush. Phys. Rev. E 2002, 65(3), 30802.
31 Suo, T.; Whitmore, M. D. Self-consistent field theory of tethered polymers: One dimensional, three dimensional, strong stretching theories and the effects of excluded-volume-only interactions. J. Chem. Phys. 2014, 141(20), 204903.
32 Meng, D.; Wang, Q. Solvent response of diblock copolymer brushes. J. Chem. Phys. 2009, 130(13), 134904.
33 Trefethen, L. N., "Spectral methods in MATLAB", SIAM, Philadelphia, 2000.
34 Douglas, J. F.; Nemirovsky, A. M.; Freed, K. F. Polymer-polymer and polymer-surface excluded volume effects in flexible polymers attached to an interface: comparison of renormalization group calculations with Monte Carlo and direct enumeration data. Macromolecules 1986, 19(7), 2041−2054.
35 Wu, D. T.; Fredrickson, G. H.; Carton, J. P. Surface segregation in conformationally asymmetric polymer blends: Incompressibility and boundary conditions. J. Chem. Phys. 1996, 104(16), 6387−6397.
36 Hur, S. M.; Garca-Cervera, C. J.; Fredrickson, G. H. Chebyshev collocation in polymer field theory: application to wetting phenomena. Macromolecules 2012, 45(6), 2905−2919.
37 Laradji, M.; Guo, H.; Zuckermann, M. Off-lattice Monte Carlo simulation of polymer brushes in good solvents. Phys. Rev. E 1994, 49(4), 3199−3206.
38 de Gennes, P. G.; Pincus, P. Scaling theory of polymer adsorption: proximal exponent. J. Phys. Lett. 1983, 44(7), 241−246.
39 Chakrabarti, A.; Nelson, P.; Toral, R. Structure of polymer chains end-grafted on an interacting surface. Phys. Rev. A 1992, 46(8), 4930−4934.
40 Grest, G. S. Grafted polymer brushes: a constant surface pressure molecular dynamics simulation. Macromolecules 1994, 27(2), 418−426.
41 Flatt, R. J.; Schober, I.; Raphael, E.; Plassard, C.; Lesniewska, E. Conformation of adsorbed comb copolymer dispersants. Langmuir 2009, 25(2), 845−855.

https://doi.org/10.1007/s10118-018-2100-4